# Flexural Behavior of Asymmetric Structural Foams

**M. Reza Barzegari, Denis Rodrigue**

*Department of Chemical Engineering and CERMA, Université Laval, Quebec City QC, Canada G1V 0A6*

Received 21 November 2008; accepted 25 February 2009
DOI 10.1002/app.30335
Published online 4 May 2009 in Wiley InterScience (www.interscience.wiley.com).

**ABSTRACT:** Asymmetric structural foams were prepared by compression molding to study the flexural properties of these sandwich structures with different layer thickness. It was found that the flexural properties of asymmetric structural foams are function of load direction. Since the bending behavior is a combination of tension and compression, the stress distribution across the foam core plays a key role in describing their bending properties. The experimental results show that the compression modulus of integral foams is lower than its tensile modulus. Based on this information, a model is proposed to predict the flexural properties of asymmetric structural foams based on stress distribution.  J Appl Polym Sci 113: 3103–3112, 2009

**Key words:** flexion; tension; compression; structural foams; skin thickness

## INTRODUCTION

Sandwich structures are multilayer materials used mostly when flexural loading are predominant. The overall behavior of a three-layer structure is determined by the global stiffness of each component: the skins and the core. This sandwich combination results in higher specific mechanical properties (strength to weight ratio), especially when the core section is foamed.[1–3] This led to the development of structural foams.

In reality, the bending modulus of a material is a macroscopic property combining the tensile and compression properties of each component under specific loading conditions. Numerous works have been reported on the mechanical properties of symmetric structural foams, i.e., when the skins are made of the same material and are of equal thickness. In these cases, it is generally assumed that the tension and compression moduli are equal in the calculations.[1,2,4–7] Theoretical and experimental results showed that for symmetric structural foams, the mechanical properties are mainly dependent on density reduction, density distribution, and skin thickness.[1,2,4–8] Unfortunately, very few works investigated the flexural properties of asymmetric structural foams, i.e., when the skins are made of different materials or having different thickness.[9–12] In this special case, all the results indicated that the apparent flexural modulus is a function of the side on which the load is applied. The origin of this difference must be linked to the stress distribution inside the beam that goes from compression to tension between the top and bottom face of the beam.

In the past, several authors studied the difference between tension and compression modulus as a particular case of nonsymmetric stress–strain behavior for composite specimen under flexural loads.[13–16] Mujika et al.[13] described an experimental procedure to obtain the ratio between tensile and compression modulus of fiber reinforced composites using four point and three point flexural tests with strain gauges. Their results showed that the tensile modulus was higher than the compression modulus and the relative difference is about 5%. Similarly, Rodrigue and co-workers studied the flexural properties of symmetric and asymmetric high-density polyethylene (HDPE) and low-density polyethylene (LDPE) structural foams produced by injection and compression molding.[10–12] Their results clearly showed that for symmetric structural foams, the apparent flexural modulus was the same irrespective of the side on which the load was applied on. On the other hand, for asymmetric structural foams, the apparent flexural modulus was higher when the load was applied on the thicker skin side. For the moment, several models are available to predict the flexural modulus of symmetric foams with high precision.[4–7] Unfortunately, the same cannot be said for asymmetric ones.

In the present work, a focus is made on the flexural properties of asymmetric structural foams. After a short review of the existing models, a description of the experimental work is presented. Finally, a model is proposed to predict the apparent flexural

*Correspondence to:* D. Rodrigue (Denis.Rodrigue@gch.ulaval.ca).

Contract grant sponsor: Natural Sciences and Engineering Research Council of Canada.

modulus of asymmetric structural foams as a function of the applied load condition.

## Mechanical modeling of cellular materials

Several models have been developed to predict the mechanical properties of cellular materials as a special case of composite materials. The mechanical properties of uniform (integral) foams are strongly related to foam density. Cell geometry and structure are also important, especially for low-density cellular materials.[1,4]

Several density-dependent equations have been proposed to describe the mechanical behavior of foams.[1,4,17–21] The empirical power–law relationship is the simplest stating that:[4,18]

$$\frac{M_f}{M_m} = C\left(\frac{\rho_f}{\rho_m}\right)^n \tag{1}$$

where $M$ is any specific property such as shear, bulk, or Young's modulus and $\rho$ is density. The subscripts $m$ and $f$ represent the unfoamed (matrix) and foamed property, respectively. $C$ and $n$ are constants related to the specific mechanical property to be predicted, as well as applied load, cell geometry and spatial arrangement, Poisson ratio, etc. The empirical square power–law of Moore and Iremonger is obtained by setting $n = 2$ and $C = 1$ in eq. (1).[22] Later, Rusch[19] presented several theoretical and empirical models for the mechanical properties of high-density foams as a function of density. Cell geometry and orientation was also added by some authors as micromechanical models.[20–22] The deformation analysis of a unit cell under loading led to the model of Gibson and Ashby[20] for the modulus $E$ as:

$$\frac{E_f}{E_m} = \phi^2\left(\frac{\rho_f}{\rho_m}\right)^2 + (1-\phi)\left(\frac{\rho_f}{\rho_m}\right) + \frac{p_o(1-2\nu_m)}{E_m\left(1-\frac{\rho_f}{\rho_m}\right)} \tag{2}$$

where $\phi$, $p_o$, and $\nu_m$ are the fraction of solid material in the cell struts, the internal gas pressure, and matrix Poisson ratio, respectively. In eq. (2), the mechanical property is controlled by three terms: the contribution of the cell struts, cell walls, and internal gas pressure. Since the internal gas pressure is generally much less than the matrix Young's modulus, the last term in eq. (2) can be neglected for rigid foams. The value of $\phi$ for closed cell foams varies between 0.6 and 0.8 (20–40% of solid in the cell faces). For $\phi = 1$, the model simplifies to the simple square power–law of eq. (1).

Because of the stress distribution inside the beam under flexion, a combination of tension and compression stresses make the prediction of bending properties more complex, especially for nonhomogeneous multiphase materials. Therefore, it is clear that the nonuniform density distribution inside structural foams, especially for the asymmetric case, needs more consideration to describe completely the flexural behavior. Nevertheless, for the symmetric case, several articles have been published with very good prediction.[4–7] This is mainly possible through the knowledge of the density distribution across the foam thickness where a single continuous and continuously differentiable equation was proposed to fit the density profile across the structural foams thickness as:[4]

$$\frac{E_f}{E_m} = \int_A \left[R_c + \frac{1-R_c}{\left[1+\left(\frac{y}{b_1}\right)^{-c_1}\right]^{d_1}}\right]^n dA \tag{3}$$

where $b_1$, $c_1$, and $d_1$ are three parameters used to fit the density profile and $R_c$ is the relative core density defined by:

$$R_c = \rho_c/\rho_m \tag{4}$$

where $\rho_c$ represented the minimum density in the core (centerline).

For asymmetric structural polymer foams, the apparent flexural modulus difference between both sides of the beam was reported by Chen and Rodrigue.[11] They found that the flexural modulus asymmetry ratio ($E_1/E_2$) is linearly proportional to the skin thickness ratio and to the square of the core void fraction to give:

$$\frac{E_1}{E_2} - 1 = \left(1-\frac{s_2}{s_1}\right)\left(1-\frac{\rho_c}{\rho_m}\right)^2 \tag{5}$$

where $s_1$ and $s_2$ are the thickness of the lower and upper skins. $E_1$ and $E_2$ are the resulting apparent flexural moduli when the load is applied on the $s_1$ or $s_2$ direction, respectively. Although this model estimates the flexural modulus ratio, it cannot describe the individual values of both moduli. To do so, one must consider that the mechanical behaviour of the foam is different than its unfoamed counterpart. Furthermore, different amounts of foamed and unfoamed materials are in tensile or compression states due to variation in stress distribution inside the beam in relation with the position of the neutral axis as presented in Figure 1. An attempt to predict the apparent flexural modulus for asymmetric structural foams is presented next with support from experimental data.

## Bending stresses in composite beams

The deflection of a beam under a three-point bending test is based on several assumptions. The plane cross-sections of the beam remain planar and normal to the longitudinal direction of the beam after

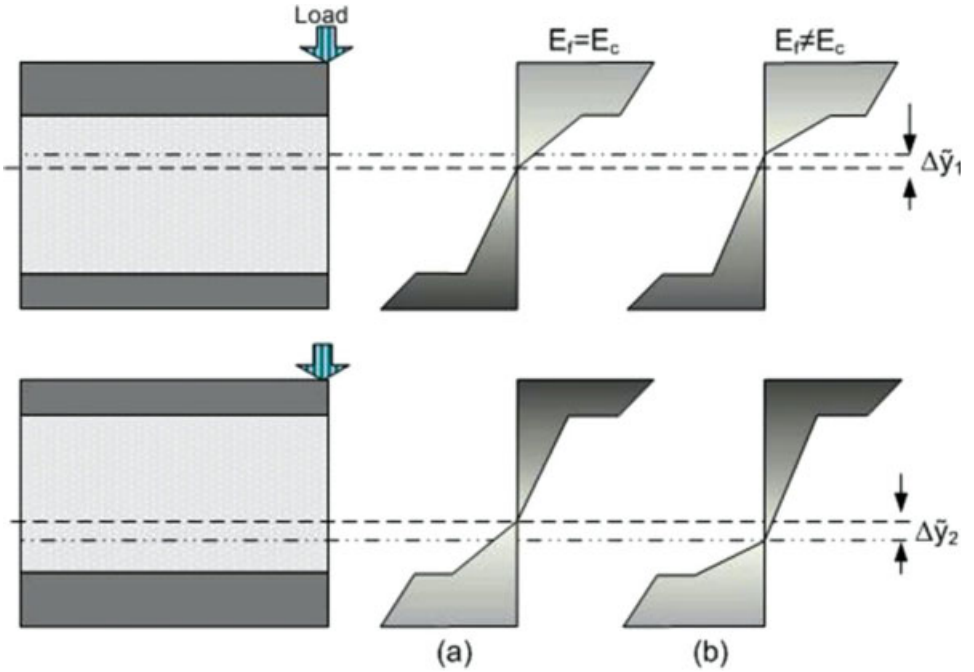


**Figure 1** Schematic representation of the stress distribution in asymmetric structural foams when the compression and tension modulus are (a) equal and (b) unequal. [Color figure can be viewed in the online issue, which is available at www.interscience.wiley.com.]

bending and the beam behavior is linear elastic.[16] The deflection is assumed to be small to eliminate the effect of creep and shear inside the beam. For a rectangular cross-section, it is assumed that the longitudinal normal strain ($\varepsilon$) at a distance ($y$) from the neutral surface is:

$$\varepsilon = \frac{y}{R} \tag{6}$$

where $R$ and $y$ are the radius of curvature of the neutral axis and the vertical coordinate measured from the neutral surface. When bending occurs, the beam is subjected to both tensile ($\sigma_t$) and compressive ($\sigma_c$) stresses simultaneously below and above the neutral surface (Fig. 1). The tension and compression properties can be determined by the position from the neutral axis and the radius of curvature. By using equilibrium conditions of the resultant force acting over the cross-section, the neutral axis and bending moment ($M$) are determined as:[16,23]

$$\int_A \sigma dA = \int_{A_t} \sigma_t dA + \int_{A_c} \sigma_c dA = 0 \tag{7}$$

$$M = \int_A \sigma y dA = \int_{A_t} \sigma_t y dA + \int_{A_c} \sigma_c y dA \tag{8}$$

where $A$ is the surface area, and indices $c$ and $t$ represent compressive and tensile properties, respectively. By using Hooke's law, eqs. (7) and (8) for the neutral axis and bending moment of a rectangular beam of width $b$ can be written as:[16,23]

$$\int_A \sigma dA = \frac{bE_t}{R}\int_{A_t} y dy + \frac{bE_c}{R}\int_{A_c} y dy = \frac{b}{R}(E_t I + E_c I) = 0 \tag{9}$$

$$M = \frac{bE_t}{R}\int_{A_t} y^2 dy + \frac{bE_c}{R}\int_{A_c} y^2 dy \tag{10}$$

where $I$ represents the second moment of inertia. The product $EI$ is called the stiffness or rigidity of the beam.

## EXPERIMENTAL

### Polymer and polymer preparation

The polymer used in this study was Novapol LA-0219-A (Nova Chemicals, Canada), an LDPE with a density of 920 kg/m$^3$ and a melt index of 2.3 g/10 min at 190°C and 2.16 kg (ASTM D1238). All the foams were produced using a modified grade of azodicarbonamide: Celogen 754-A (Crompton Chemicals). This chemical blowing agent has a decomposition temperature range between 165 and 180°C. The components were first blended using a laboratory internal mixer (Haake Rheomix) at 40 rpm and 130°C and the amount of blowing agent was set

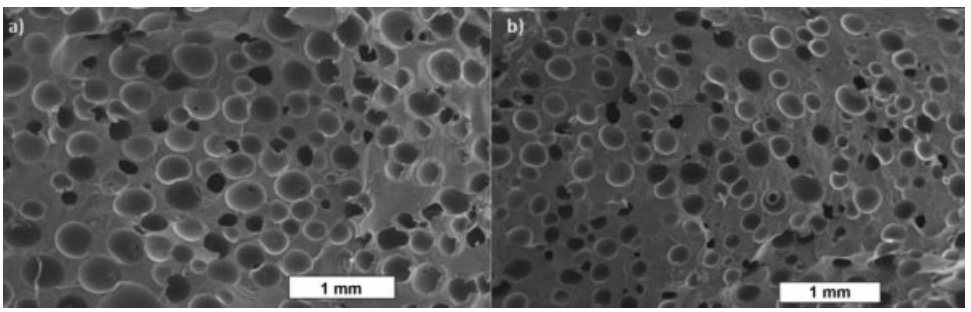


**Figure 2** Typical SEM micrographs of LDPE uniform foams (IF) produced by compression molding.

between 1 and 2 wt %. Then, LDPE structural foams were produced by a sandwich compression molding technique. The blends were used to produce unfoamed rectangular plates with different thickness at 140°C. Then, one unfoamed blend plate with blowing agent (to form the core) was placed between two LDPE plates of similar or different thicknesses (to form the skins) to produce symmetric and asymmetric structural foams, respectively. The two steps sandwich molding process was then used. First, preheating was done at 140°C for 4 min and compression was applied at 170°C and 10 MPa for 3 min. Then, the pressure was removed gradually and the mold was cooled down to 60°C with circulating water. Further details on foam preparation can be found elsewhere.[4,11] Uniform integral foams were also produced. In this case, the unfoamed blend with blowing agent was placed alone in a rectangular mold of varying thickness (2.5–4 mm) at 170°C for 3 min to expand and produce foamed samples of different density. The mold was cooled down to 60°C with circulating water and opened to retrieve the foamed samples.

### Morphology analysis

Morphological characterization of the foams was obtained from a stereomicroscope (Olympus SZ-PT) coupled with a digital camera (Spot Insight). Skin thickness and cell diameter ($d$) was determined using Image-Pro Plus 4.5 (Media Cybernetics). The average of a minimum of 300 cells is reported with the standard deviation. Skin thickness was calculated by the distance between the surface and the closest cells at different locations to get the average. The evaluation was performed on both sides of each sample to verify the asymmetry, to get the total skin thickness and to calculate the skin ratio defined as the total skin thickness divided by the total sample thickness. Further analyses were performed on micrographs taken on a scanning electron microscope (SEM) JEOL model JSM-849. The structure of the foams was exposed through cryogenic fracture and coated with a thin layer of Au/Pd before analysis.

### Flexural measurements

Determination of the flexural modulus was performed on an Instron universal tester model 5565 with a 50 N load cell according to ASTM D790. The samples (60 × 12.7 mm) were cut from the rectangular molded plates. Three point bending tests were carried out at a rate of 5 mm/min at room temperature. The modulus of elasticity ($E$) is calculated experimentally by (ASTM D790):

$$E = \frac{L^3 m}{4bd^3} \tag{11}$$

where $m$ is the slope of the initial linear portion of the load-deflection curve. The parameters $L$, $b$, and $d$ are the support span, width of beam, and depth of beam, respectively. At least three samples were used to report the average and standard deviation for each side. The results are reported as normalized values with respect to the unfoamed LDPE matrix (205.5 ± 7.7 MPa).

### Tensile and compression measurements

For modeling purposes, tensile and compression moduli were also determined on an Instron universal tester model 5565 with 50 and 500 N load cells. The tensile samples were cut from the molded plates according to ASTM D638 (Type V). The compression test samples were cut with dimensions of 2 × 2 × 1.5 cm. Both types of measurements were carried out at a rate of 5 mm/min at room temperature. The results are reported as the average and standard deviation of at least three samples and normalized with respect to the unfoamed LDPE modulus (129.3 ± 8.2 MPa).

## RESULTS AND DISCUSSION

As described in the experimental section, three sets of samples including symmetric structural foam (SF), asymmetric structural foam (AF), and integral foam (IF) samples were prepared in this work. Figures 2 and 3 show typical SEM micrographs of the

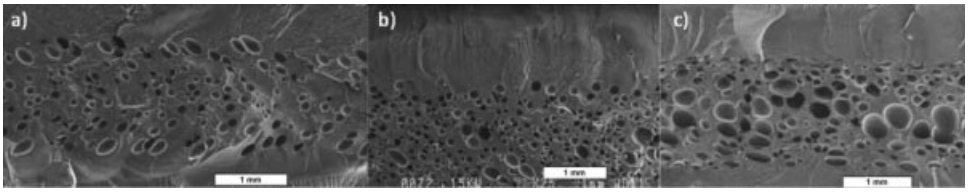


**Figure 3** Typical SEM micrographs of symmetric (a) and asymmetric (b,c) LDPE structural foams.

samples. Different skin thickness on both sides can be clearly seen in these micrographs and Table I reports on the morphological characterization the structural foams (SF-1 to SF-4 and AF-1 to AF-6). It can be seen that a wide range of conditions were produced where density reduction up to 22% and total skin thickness ratio up to 38% were obtained. As a first approximation, the density of the core section ($\rho_c$) is assumed constant (equivalent weight) and can be calculated by a simple mass balance using the skin thickness as:[4]

$$\rho_f \delta_f = \rho_c(\delta_f - \delta_{st}) + \rho_s \delta_{st} \tag{12}$$

where $\delta_{st}$ is the total skin thickness ($\delta_{st} = \delta_{s1} + \delta_{s2}$). The normalized core density is given by:

$$\frac{\rho_c}{\rho_s} = \left(\frac{\rho_f}{\rho_s} - \frac{\delta_{st}}{\delta_f}\right)\left(1 - \frac{\delta_{st}}{\delta_f}\right)^{-1} \tag{13}$$

As presented in a previous study,[17] it is possible to produce almost skinless foams of uniform density (constant density profile) by compression molding. From this technique, several samples were produce to compare their mechanical behavior under compression and tension loading. Morphological analysis of these LDPE integral foam (IF) was performed and typical SEM micrographs are presented in Figure 2 where skins are almost inexistent.

The morphological characterization and compressive modulus of the integral foam samples are reported in Table II where a wide range of relative foam density (0.403–0.768) has been produced. As expected, Table II shows that the compressive modulus decreases with decreasing foam density. To better understand the mechanical behavior of asymmetric structural foam, the tension and compression stress–strain curves of integral foam are analyzed next.

### Tension and compression behavior of integral foams

Typical compression stress–strain curves for LDPE integral foams are shown in Figure 4. The compressive strain–stress behavior of all the samples shows a linear part at low stresses. Then, the behavior is characterized by deformation at relatively constant stress where the cell walls collapse. The final section of the curve is densification where the foam begins to respond as a compacted solid because the cellular structure has collapsed and further deformation requires compression of the solid matrix material.[24] As seen in Figure 4, increasing the foam density increases the modulus and plateau stress level, but decreases the strain at which densification occurs due to lower amount of material composing the cell walls.

Typical stress–strain curves for unfoamed and foamed LDPE sample in compression and tension are compared in Figure 5(a,b). Figure 5(a) shows that for unfoamed LDPE samples, similar tension and compression modulus are obtained. On the other hand, Figure 5(b) shows that this is not the case for foamed samples. One way to represent and quantify this difference between tensile and compression moduli is by the power-law of eq. (1). As

**TABLE I**
**Foam Characteristics of SF and AF Samples (Normalized Values)**

| Sample | Relative density | $s_1$ | $s_2$ | Relative core density | Average cell diameter (μm) |
|---|---|---|---|---|---|
| SF-1 | 0.791 ± 0.007 | 0.157 | 0.156 | 0.696 | 144 ± 28 |
| SF-2 | 0.813 ± 0.003 | 0.178 | 0.173 | 0.712 | 149 ± 32 |
| SF-3 | 0.845 ± 0.006 | 0.168 | 0.166 | 0.768 | 122 ± 14 |
| SF-4 | 0.859 ± 0.004 | 0.155 | 0.151 | 0.797 | 176 ± 31 |
| AF-1 | 0.854 ± 0.004 | 0.296 | 0.137 | 0.742 | 171 ± 81 |
| AF-2 | 0.821 ± 0.008 | 0.395 | 0.050 | 0.700 | 233 ± 92 |
| AF-3 | 0.782 ± 0.005 | 0.291 | 0.117 | 0.632 | 166 ± 71 |
| AF-4 | 0.898 ± 0.003 | 0.376 | 0.192 | 0.763 | 89 ± 13 |
| AF-5 | 0.885 ± 0.003 | 0.414 | 0.073 | 0.776 | 95 ± 18 |
| AF-6 | 0.876 ± 0.005 | 0.211 | 0.153 | 0.805 | 138 ± 32 |

**TABLE II**
**LDPE Integral Foams Characterization (Compression Molded)**

| Sample | Relative density | Average cell diameter (μm) | Compressive modulus (MPa) | Relative modulus |
|---|---|---|---|---|
| IF-1 | 0.403 ± 0.006 | 256 ± 67 | 17.9 ± 3.1 | 0.139 ± 0.024 |
| IF-2 | 0.442 ± 0.011 | 263 ± 61 | 19.1 ± 2.7 | 0.148 ± 0.021 |
| IF-3 | 0.527 ± 0.009 | 218 ± 54 | 36.5 ± 3.7 | 0.282 ± 0.028 |
| IF-4 | 0.618 ± 0.012 | 233 ± 49 | 45.4 ± 4.8 | 0.351 ± 0.037 |
| IF-5 | 0.699 ± 0.008 | 189 ± 41 | 50.7 ± 6.4 | 0.392 ± 0.050 |
| IF-6 | 0.768 ± 0.007 | 178 ± 45 | 64.5 ± 7.7 | 0.499 ± 0.061 |

mentioned previously, the simple power-law equation is quite popular to predict the relation between mechanical properties and foam density. The exponent $n$ is related to the type of mechanical property such as tension and compression as well as foam morphology, Poisson ratio, etc. In this case, a single parameter ($n$) is used for foams produced from a specific polymer with similar morphology (spherical cells in high-density foams).

Therefore, the value of $n$ was obtained by fitting eq. (1) to the relative compression moduli reported in Table III using the nonlinear regression package of SigmaPlot 8.0. As presented in Figure 6, the best value was found to be $n = 2.29 \pm 0.08$ with $R^2 = 0.982$, which is close to $n = 2$ of the empirical square power-law. Tensile behavior of integral and structural foams has been studied in our earlier studies.[17] Using the same approach for the tensile modulus, $n$ was found to be $1.91 \pm 0.06$ with $R^2 = 0.982$, for this particular LDPE.[17] Statistically different $n$ values for tension and compression indicates the possibility that foams have different tensile and compression moduli as reported elsewhere.[1,25]

## Flexural modulus

Figure 7(a,b) presents typical stress–strain curves for symmetric and asymmetric structural foams (SF-2 and AF-2), respectively. As for all our asymmetric samples, a difference was observed between the load applied on the thicker or thinner skin side of the beam [Fig. 7(b)] while symmetric samples showed similar behaviors by changing the direction of applied load [Fig. 7(a)]. Table III reports that the flexural properties for the symmetric case are very close to each other within experimental uncertainty. On the other hand, a clear difference between the flexural modulus of asymmetric structural foams is obtained by changing the direction of applied load. Table III also indicates that higher apparent flexural moduli were obtained when the load was applied on the thicker side and this result is similar as reported by Chen and Rodrigue[11] on LDPE structural foams produced by compression molding and Tovar-Cisneros et al.[10] for HDPE foams produced by injection molding.

To develop a model for flexural properties of asymmetric structures, it is proposed to decompose the composite beam into four parts: the skin and core sections on both sides of the neutral axis. A schematic representation with the nomenclature used is given in Figure 8.

As mentioned previously in eq. (9), the neutral axis is located where the resultant force acting on the cross-section is zero. An integration of the compressive and tensile forces over the upper and lower sections of the beam gives:

$$\left(E_{f_1}\right)_t \int_0^{h_1} y dy + \left(E_{s_1}\right)_t \int_{h_1}^{h_1+s_1} y dy - \left(E_{f_2}\right)_c \times \int_0^{h_2} y dy - \left(E_{s_2}\right)_c \int_{h_2}^{h_2+s_2} y dy = 0 \quad (14)$$

where $s_1$ and $s_2$ are the lower and upper relative skin thickness, respectively. The parameters $h_1$, $h_2$, and $h$ ($= h_1 + h_2$) are the core thickness below the neutral axis, core thickness above the neutral axis,

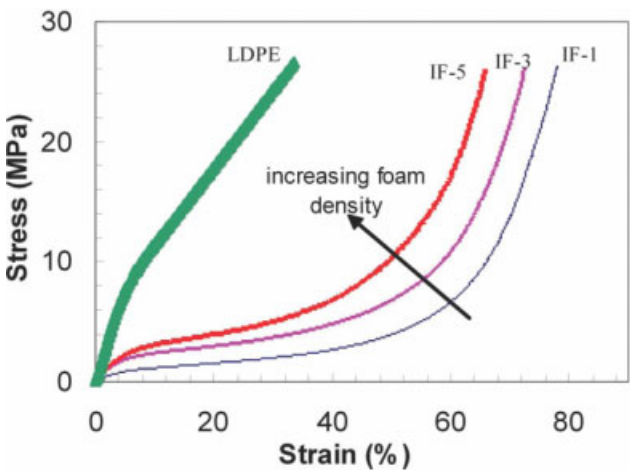


**Figure 4** Compressive stress–strain curves for LDPE and three integral foams of different densities. [Color figure can be viewed in the online issue, which is available at www.interscience.wiley.com.]

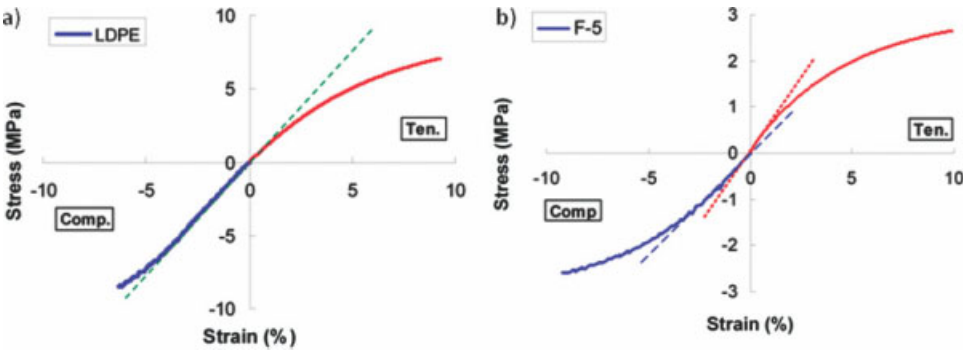


**Figure 5** Typical stress–strain curves for (a) unfoamed and (b) foamed LDPE samples. The dotted and dashed lines represent the slope of the tensile and compression stress–strain curve, respectively. [Color figure can be viewed in the online issue, which is available at www.interscience.wiley.com.]

**TABLE III**
**Relative Flexural Modulus of SF and AF Samples (Normalized Values)**

| Sample | Relative density | $E_1$ | $E_2$ | $E_{ave.}$ | $E_2/E_1$ |
|---|---|---|---|---|---|
| SF-1 | 0.791 | 0.773 ± 0.006 | 0.765 ± 0.010 | 0.769 | 0.989 ± 0.021 |
| SF-2 | 0.813 | 0.818 ± 0.012 | 0.812 ± 0.007 | 0.815 | 0.992 ± 0.023 |
| SF-3 | 0.845 | 0.851 ± 0.012 | 0.858 ± 0.016 | 0.845 | 0.991 ± 0.033 |
| SF-4 | 0.859 | 0.911 ± 0.009 | 0.907 ± 0.015 | 0.909 | 0.995 ± 0.026 |
| AF-1 | 0.854 | 0.906 ± 0.012 | 0.820 ± 0.013 | 0.863 | 0.905 ± 0.029 |
| AF-2 | 0.821 | 0.737 ± 0.011 | 0.614 ± 0.007 | 0.675 | 0.832 ± 0.026 |
| AF-3 | 0.782 | 0.878 ± 0.012 | 0.785 ± 0.018 | 0.831 | 0.894 ± 0.037 |
| AF-4 | 0.898 | 0.910 ± 0.010 | 0.873 ± 0.013 | 0.892 | 0.958 ± 0.026 |
| AF-5 | 0.885 | 0.887 ± 0.013 | 0.809 ± 0.016 | 0.848 | 0.912 ± 0.034 |
| AF-6 | 0.876 | 0.868 ± 0.015 | 0.842 ± 0.012 | 0.865 | 0.969 ± 0.031 |

and total core thickness, respectively. The parameter $H$ is the total foam thickness which is considered as unity in this work. $(E_{f_1})_t$, $(E_{f_2})_c$, $(E_{s_1})_t$, and $(E_{s_2})_c$ are the modulus of the foam core below the neutral axis (part 1) in tension, modulus of the foam core above the neutral axis (part 2) in compression, modulus of the skin below the neutral axis (part 1) in tension, and modulus of the skin above the neutral axis (part 2) in compression, respectively. Equation (14) assumes that the modulus of each section is constant due to constant local density. It can also be written as

$$H = h + s_1 + s_2 = h_1 + h_2 + s_1 + s_2 = 1 \qquad (15)$$

and

$$\frac{(E_{s_2})_c}{E_s} = \frac{(E_{s_1})_t}{E_s} = 1 \qquad (16)$$

Equation (15) is simply a geometrical relation from Figure 8 and eq. (16) states that the moduli of the skins are taken as the moduli of the unfoamed polymer. It is also assumed that for the unfoamed polymer, the tensile and compressive moduli are equal: $E_s = (E_s)_c = (E_s)_t$ as shown in Figure 5.

## Equal foam moduli for compression and tension

If the compression and tension moduli of the foamed sections are equal, this gives $(E_f)_c = (E_f)_t = E_f$. In this case, the value of $h_1$ and $h_2$ are calculated by solving simultaneously eqs. (14)–(16) to give:

$$h_1 = \frac{(s_1+s_2)^2(1-\bar{E}_f) - \bar{E}_f\left(H^2 - 2H(s_1+s_2)\right) - 2Hs_2}{2\left(\bar{E}_f(s_1+s_2-H) - (s_1+s_2)\right)} \qquad s_1, s_2 < \bar{y} \qquad (17)$$

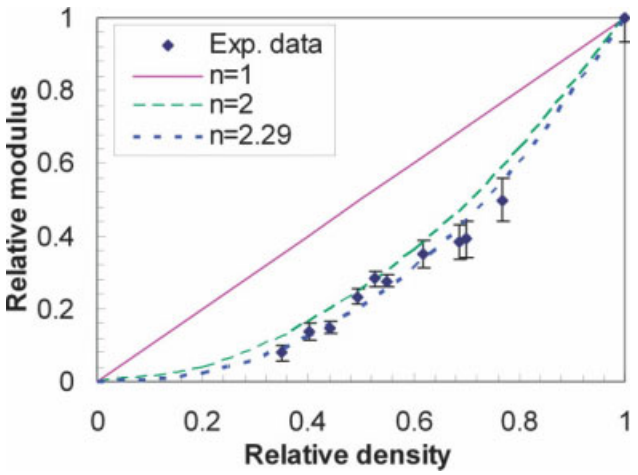


**Figure 6** Relative compression modulus as a function of relative density for LDPE uniform foams and compared with eq. (1) using $C = 1$ and $n = 1$, 2, or 2.29. [Color figure can be viewed in the online issue, which is available at www.interscience.wiley.com.]

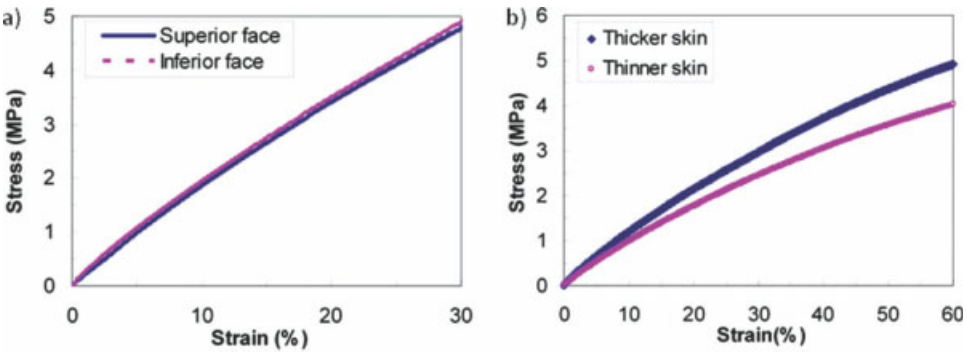


**Figure 7** Flexural behavior of (a) SF-3 and (b) AF-2 when the load was applied on the thicker or thinner side. [Color figure can be viewed in the online issue, which is available at www.interscience.wiley.com.]

where $\bar{E}_f$ is the relative foam modulus. The parameter $\bar{y}$ is the position of the neutral axis that can be obtained by the summation of $h_1$ and $s_1$ from the bottom side of the beam:

$$\bar{y} = h_1 + s_1 \tag{18}$$

The relative apparent flexural modulus of a sandwich structure is obtained by dividing the structural foam modulus ($E_{sf}$) by the modulus of the solid polymer beam of uniform modulus ($E_m$) as:

$$\frac{E_{sf}}{E_m} = \frac{\int_A E_y y^2 dA}{E_m I_y} = \frac{12}{H^3}\int_A \left(\frac{E_f}{E_m}\right) y^2 dA$$
$$= \frac{4}{H^3}\left(\frac{(E_{f_2})_c}{E_m}h_2^3 + \frac{(E_{m_2})_c}{E_m}\left((h_2+s_2)^3 - h_2^3\right) + \frac{(E_{f_1})_t}{E_m}h_1^3 + \frac{(E_{m_1})_t}{E_m}\left((h_1+s_1)^3 - h_1^3\right)\right) \tag{19}$$

Taking here the same value for the compression and tension moduli (which are function of foam density) as:

$$\frac{(E_{f_2})_c}{E_m} = \frac{(E_{f_1})_t}{E_m} = \beta = \left(\frac{\rho_c}{\rho_m}\right)^2 \tag{20}$$

The relative flexural modulus for the asymmetric structural foam can be obtained from eqs. (19)–(20) as:

$$\frac{E_{sf}}{E_m} = \frac{4}{H^3}\left((h_1^3 + h_2^3)(\beta - 1) + \left((h_1+s_1)^3 + (h_2+s_2)^3\right)\right) \tag{21}$$

Unequal foam moduli for compression and tension

By considering a different value for the compression and tension foam moduli:

$$\frac{(E_{f_2})_c}{E_s} \neq \frac{(E_{f_1})_t}{E_s} \tag{22}$$

The value of $h_1$ and $h_2$ are calculated by solving simultaneously eqs. (14)–(16) and (22) to give:

$$h_1 = \left(\frac{1}{\bar{E}_{f,t} - \bar{E}_{f,c}}\right)\left(\bar{E}_{f,c}(\lambda - H) - \lambda\right) + \left(\lambda^2 + \left(1 - \bar{E}_{f,t} + \bar{E}_{f,t}\bar{E}_{f,c} - \bar{E}_{f,c}\right) - \left(\bar{E}_{f,t}\bar{E}_{f,c}H(2\lambda - H)\right) + 2H\left(\bar{E}_{f,c}s_1 + \bar{E}_{f,t}s_2\right)\right)^{1/2} \qquad s_1, s_2 < \bar{y} \tag{23}$$

where $\bar{E}$ is the relative value for the modulus (modulus of the foam divided by the modulus of the matrix) and $\lambda$ is the total skin thickness as:

$$\lambda = s_1 + s_2 \tag{24}$$

The relative apparent flexural modulus for the asymmetric structural foam is now given by:

$$\frac{E_{sf}}{E_m} = \frac{4}{H^3}\left(\bar{E}_{f,c}h_2^3 + (h_2+s_2)^3 - h_2^3 + (h_1+s_1)^3 - h_1^3 + \bar{E}_{f,t}h_1^3\right) \tag{25}$$

By introducing a parameter ($\alpha$) as the modulus ratio:

$$\alpha = \frac{\bar{E}_{f,c}}{\bar{E}_{f,t}} = \frac{\left(\rho_{c,c}/\rho_m\right)^{2.29}}{\left(\rho_{c,t}/\rho_m\right)^{1.91}} \tag{26}$$

The flexural modulus of asymmetric structural foams given by eq. (25) is illustrated in Figure 9(a,b)

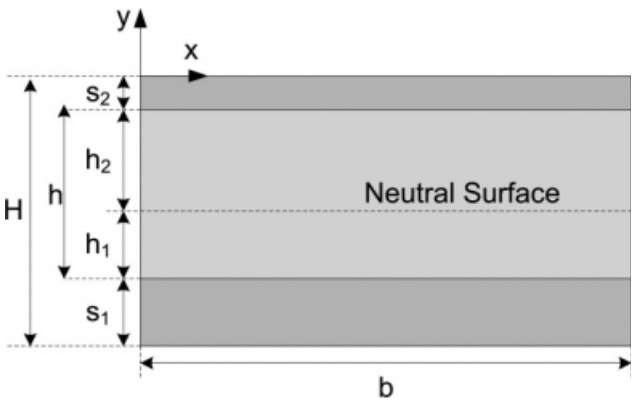


**Figure 8** Nomenclature used for modeling the flexural properties of asymmetric structural foams.

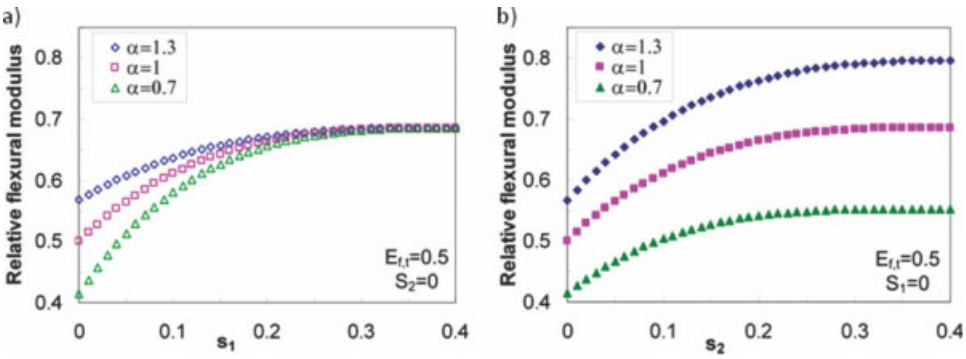


**Figure 9** Relative flexural modulus calculated by eq. (25) as a function of skin thickness (a) $s_1$ and (b) $s_2$. [Color figure can be viewed in the online issue, which is available at www.interscience.wiley.com.]

by assuming $\bar{E}_{f,t} = 0.5$ and for loads applied on the upper side. This figure shows that the flexural behavior is independent of the applied load direction for the case of $\alpha = 1$ (equal tensile and compression moduli). On the other hand, for $\alpha \neq 1$, the flexural properties are strongly function of the applied load direction. Since different amounts of foamed and unfoamed materials are in tensile or compression states depending on the loading direction, unequal value for the tensile and compression moduli leads to differences in the neutral axis position with respect to the applied load direction and this may explain the results of Figure 9(a,b). These figures also show that flexural modulus is higher when the bending load is applied on the thicker skin side [Fig. 9(b)].

Finally, the experimental data were compared with the predictions of eqs. (21) and (25) and the results are reported in Tables IV and V. Table IV shows that considering unequal tensile and compression modulus, the position of the neutral axis ($\bar{y}$), and the flexural modulus changes with the applied load direction, while the values are constant for eq. (21). The foam tensile and compression moduli of eq. (25) were calculated by the simple power-law equation of eq. (1) using $n = 1.91$ and 2.29, respectively, as presented in eq. (26). Then, the obtained value for the compression and tensile modulus were used to calculate α. Values between 0.839 and 0.920 were obtained for the range of densities studied. According to this approach, the value of α can also be calculated using the experimental compression and tensile modulus reported by Throne[1] for HDPE and PP structural foams to give $\alpha = 0.54$. For eq. (21), the foam modulus was obtained using $n = 2$ based on our previous work.[8]

Table V shows the flexural modulus deviation between the experimental data and eq. (25). The results show that the model does a relatively very good job to evaluate the flexural behavior according to the applied load direction. Table V also presents the ratio of flexural modulus of each side to compare with the model reported by Chen and Rodrigue.[11] The flexural modulus ratio ($E_2/E_1$) between the experimental data, eqs. (25) and (5) indicates a good prediction of flexural modulus.

**TABLE IV**
**Experimental Data and Model Prediction for the Structural Foams**

| | Experimental data | | Eq. (21) | | Eq. (25) | | | | |
|---|---|---|---|---|---|---|---|---|---|
| Sample | $E_1$ | $E_2$ | $\bar{y}_1$ | $E^*$ | $\bar{y}_1$ | $E_1$ | $\bar{y}_2$ | $E_2$ | $E_2/E_1$ |
| SF-1 | 0.773 | 0.765 | 0.5 | 0.832 | 0.493 | 0.826 | 0.494 | 0.826 | 1.000 |
| SF-2 | 0.818 | 0.812 | 0.5 | 0.865 | 0.493 | 0.86 | 0.496 | 0.86 | 1.000 |
| SF-3 | 0.858 | 0.851 | 0.5 | 0.878 | 0.494 | 0.873 | 0.496 | 0.873 | 1.000 |
| SF-4 | 0.911 | 0.907 | 0.5 | 0.877 | 0.495 | 0.872 | 0.496 | 0.872 | 1.000 |
| AF-1 | 0.906 | 0.820 | 0.474 | 0.896 | 0.468 | 0.894 | 0.524 | 0.881 | 0.985 |
| AF-2 | 0.737 | 0.614 | 0.417 | 0.697 | 0.401 | 0.696 | 0.582 | 0.644 | 0.925 |
| AF-3 | 0.878 | 0.785 | 0.454 | 0.831 | 0.444 | 0.829 | 0.544 | 0.809 | 0.976 |
| AF-4 | 0.910 | 0.873 | 0.480 | 0.904 | 0.476 | 0.945 | 0.519 | 0.937 | 0.992 |
| AF-5 | 0.887 | 0.809 | 0.458 | 0.862 | 0.45 | 0.862 | 0.542 | 0.838 | 0.972 |
| AF-6 | 0.868 | 0.842 | 0.492 | 0.908 | 0.487 | 0.904 | 0.505 | 0.898 | 0.993 |

$E^*$ is the structural foam modulus by considering equal values for the compression and tension modulus.

**TABLE V**
**Flexural Modulus Deviation (%) Between the Models and Experimental Data**

| | Relative modulus (Exp.) | | Relative modulus deviation (%) | | | |
|---|---|---|---|---|---|---|
| | | | Eq. (25) | | | Eq. (5) |
| Sample | $E_1$ | $E_2$ | $E_1$ | $E_2$ | $E_2/E_1$ | $E_2/E_1$ |
| SF-1 | 0.773 | 0.765 | 6 | 7 | 1 | 1 |
| SF-2 | 0.818 | 0.812 | 5 | 6 | 1 | 0 |
| SF-3 | 0.858 | 0.851 | 2 | 3 | 1 | 1 |
| SF-4 | 0.911 | 0.907 | −4 | −4 | 0 | 0 |
| AF-1 | 0.906 | 0.820 | −1 | 7 | 8 | 2 |
| AF-2 | 0.737 | 0.614 | −6 | 5 | 10 | [a] |
| AF-3 | 0.878 | 0.785 | −6 | 3 | 8 | −12 |
| AF-4 | 0.910 | 0.873 | 4 | 7 | 3 | −2 |
| AF-5 | 0.887 | 0.809 | −3 | 3 | 6 | −19 |
| AF-6 | 0.868 | 0.842 | 4 | 6 | 5 | 4 |
| Average | – | – | 4 | 5 | 7 | 7 |

[a] The model does not apply when the foam has no skin on both sides.

## CONCLUSION

In this study, the flexural modulus of asymmetric structural foams based on LDPE made by compression molding was investigated. First, it was found that the apparent flexural modulus depends on the load direction so that higher values were obtained when the load was applied on the thicker skin side. This behavior can be attributed to the stress distribution inside the beam. To confirm this hypothesis, the compressive properties of integral foams made by compression molding were studied in the range of relative density between 0.403 and 0.768. Using the results of our previous study on tensile properties of similar foams, the combined results show that the compression moduli of polymer foams are lower than their tensile counterparts. Based on our experimental results, the compression modulus was fitted to a simple power-law relation for which the optimum value of the exponent $n$ was found to be 2.29 $\pm$ 0.08; whereas for tension data, the value is 1.91 $\pm$ 0.08. Finally, a model was presented to predict the flexural modulus of asymmetric structural foams by taking into account the skin thickness on both sides, the stress distribution inside the beam (compression and tension), and the mechanical behavior of the integral foam core in terms of density reduction. The results show that the proposed model can predict our experimental data with an average of 5% and a maximum of 7% deviation in the range of conditions studied: relative foam density (0.782–0.898), relative core density (0.632–0.818), and relative skin thickness (0–0.414).

## References


1. Throne, J. L. Thermoplastic Foams, Sherwood Publishers: Hinckley, 1996.
2. Shutov, F. A. Integral/Structural Polymer Foams; Technology, Properties and Applications, Springer Verlag: Berlin, 1986.
3. Kaw, A. K. Mechanics of Composite Materials, CRC Press: Boca Raton, 2006.
4. Barzegari, M. R.; Rodrigue, D. Polym Eng Sci 2007, 47, 1459.
5. Zhang, Y.; Rodrigue, D.; Aït-Kadi, A. J Appl Polym Sci 2003, 90, 2139.
6. Progelhof, R. C.; Eilers, K. Soc Plast Eng. 1977, DIVTEC, Woburn.
7. Progelhof, R. C.; Throne, J. L. Polym Eng Sci 1979, 19, 493.
8. Khakhar, D. V.; Joseph, K. V. Polym Eng Sci 1994, 34, 726.
9. Vaidya, N. Y.; Khakhar, D. V. J Cell Plast 1997, 33, 587.
10. Tovar-Cisneros, C.; Gonzalez-Nuñez, R.; Rodrigue, D. Proc SPE ANTEC 2007, 2120.
11. Chen, X.; Rodrigue, D. J Cell Plast 2009, to appear.
12. Barzegari, M. R.; Rodrigue, D. Proceedings of the 24th Annual Meeting of the Polymer Processing Society (PPS-24); 2008; 15.
13. Mujika, F.; Carbajal, N.; Arrese, A.; Mondragón, I. Polym Test 2006, 25, 766.
14. Paolinelis, S. G.; Paipetis, S. A.; Theocaris, P. S. J Test Eval 1979, 7, 177.
15. Jones, R. M. J Compos Mater 1976, 10, 342.
16. Gere, J. M.; Timoshenko, S. P. Mechanics of Materials, 4th Ed.; PWS Publication: Boston, 1997.
17. Barzegari, M. R.; Rodrigue, D. Cell Polym 2008, 27, 217.
18. Avalle, M.; Belingardi, G.; Ibba, A. Int J Impact Eng 2007, 34, 3.
19. Rusch, K. C. J Appl Polym Sci 1969, 13, 2297.
20. Gibson, L. J.; Ashby, M. F. Cellular Solids: Structure and Properties, 2nd Ed.; Cambridge University Press: Cambridge UK, 1997.
21. Ramakrishnan, N.; Arunachalam, V. S. J Am Ceram Soc 1993, 76, 2745.
22. Iremonger, M. J.; Lawler, J. P. J Appl Polym Sci 1980, 25, 809.
23. Rees, D. W. A. Mechanics of Solids and Structures, Imperial College Press: UK, 2000.
24. Ouellet, S.; Cronin, D.; Worswick, M. Polym Test 2006, 25, 731.
25. Wang, B.; Peng, Z.; Zhang, Y.; Zhang, Y. J Appl Polym Sci 2007, 105, 3462.